THREE-DIMENSIONAL LARGE STRAIN ELASTO VISCOPLASTIC CONSTITUTIVE MODEL

Melisa S. Ribero Vairo[a,b]**, Claudio Careglio**[a]**, Carlos García Garino**[a,b]**, Anibal E. Mirasso**[a] **and Jean P. Ponthot**[c]

[a]*Facultad de Ingeniería, Universidad Nacional de Cuyo*

[b]*Instituto de las Tecnologías de la Información y las Comunicaciones, Universidad Nacional de Cuyo, melisaribero@yahoo.com.ar, cgarcia@itu.uncu.edu.ar*

[c]*Aerospace and Mechanical Engineering Department, University of Liège, B4000, Liège, Belgium*

Keywords: large strains, viscoplasticity, finite elements.

Abstract. In a previous work, J. Ponthot et al., *Mec Comput*, XXIV:441-454 (2005), have extended a large strain elastoplastic constitutive model based on hyperelasticity and multiplicative decomposition of deformation gradient tensor, to viscous case based on a contribution of the same main author . In this way a very useful tool has been obtained, able to deal with both rate dependent and rate independent problems.

In this work a brief review of theoretical details is presented and numerical implementation of the model in a three-dimensional finite element code (**SOGDE3D**) is performed. The finite element code was developed for solving elastoplasticity in solids under large strains in three-dimensional space.

A Newton Raphson scheme has been used to solve the non-linear consistency condition in order to compute the viscoplastic multiplier.

An analysis of large viscoplastic deformation problems under plane strain condition are provided in order to test the proposed model. A comparison between two and three-dimensional versions of **SOGDE** code is achieved to validate the implementation and some results available in the literature helped to confirm the correct recovery of elastoplastic response by the viscoplastic model.

1   INTRODUCTION

The main objective of this work is to combine a three-dimensional (3D) finite element code with a viscoplastic model. The first element in the combination is the **SOGDE3D** code, developed by Careglio et al. (2005) for solving elastoplasticity in solids under large strains in 3D space. It is based on the constitutive model due to García Garino and Oliver (1995, 1996) which has been implemented in the relative simple hexahedral linear finite element ($H1$) and the well known hexahedral linear one with constant pressure ($H1/P0$) (Zienkiewicz and Taylor (1994)).

The viscoplastic constitutive model implemented in **SOGDE3D** is a generalization of the Perzyna (1966) constitutive model due to Ponthot (2002). It was originally developed for the hypoelastic model, proposing for J2-flow materials a unified integration algorithm as an extension of the classical radial return scheme to the viscoplastic domain. In Ponthot et al. (2005) the same constitutive model was adapted for an hyperelastic material and in García Garino et al. (2006) linear viscoplasticity have been presented and discussed. Also Castelló and Flores (2010) made an implementation of the viscoplastic model, obtaining results for the same linear viscoplastic case but using a three-node triangular finite element with two degrees of freedom per node (Castelló and Flores (2008)).

In García Garino et al. (2011) the viscoplasticity model was generalized and tested for non-linear consistency equation in two-dimensional (2D) problems. At that time, the platform chosen to implement the viscoplastic model was **SOGDE2D** code (García Garino (1993)). A mathematical interpretation of viscoplastic parameters was carried out and proved in some numerical examples.

This work presents a brief review of the theoretical framework of the problem in section 2. Then the implemented numerical scheme is shown in section 3 and numerical examples as a plate with a hole (Alfano et al. (2001)) and the GRECO beam (an academic benchmark proposed by the GRECO project whose results were compiled by El Mouatassim (1989)) are analysed in section 4. Both examples are discretized on its geometry with $H1/P0$ elements. Some conclusions about the work accomplished are detailed in section 5.

2   LARGE STRAIN ELASTO/VISCOPLASTIC MODEL

2.1   Kinematics

The kinematics of the problem is based on the very well known multiplicative decomposition of the deformation gradient tensor $\boldsymbol{F}$ in its elastic and plastic components (Lee (1969)), as shown in equation (1).

$$\boldsymbol{F} = \boldsymbol{F}^e \, \boldsymbol{F}^{vp}. \tag{1}$$

An additive decomposition of the Almansi strain tensor $\boldsymbol{e}$ can be derived from the multiplicative decomposition of the deformation gradient tensor (García Garino (1993)). Viscoplastic $\boldsymbol{e}^{vp}$ and elastic $\boldsymbol{e}^e$ components can be distinguished,

$$\boldsymbol{e} = \boldsymbol{e}^e + \boldsymbol{e}^{vp} . \tag{2}$$

The total Almansi strain and its elastic component are defined in equation (3) and (4) respec-

tively.

$$e = \frac{1}{2}(g - b^{-1}), \tag{3}$$

$$e^e = \frac{1}{2}(g - b^{e-1}). \tag{4}$$

where the spatial metric tensor is denoted as g, the Finger tensor is defined as $b^{-1} = F^{-T} F^{-1}$ and its elastic component as $b^{e-1} = F^{e-T} F^{e-1}$.

The rate of the deformation tensor d is obtained computing the Lie derivative L_v (Marsden and Hughes (1983)) of Almansi strain tensor e, and admits an additive decomposition in its elastic and viscoplastic components $d = d^e + d^{vp}$.

2.2 Viscoplastic model

The equations that define the viscoplastic model in the current configuration are similar to the classic elastoplastic model, as well as the Kuhn-Tucker conditions considering an extended yield criterion $\bar{f}$ to the viscoplastic case, defined later in equation (17). Then, the model is based in the expressions listed below,

$$\sigma = \frac{\partial \psi^e(e^e, b^{e-1})}{\partial e^e}, \tag{5}$$

$$d^{vp} = \dot{\lambda}^{vp} n, \tag{6}$$

$$\dot{\lambda}^{vp} \geq 0 \quad \bar{f} \leq 0 \quad \dot{\lambda}^{vp} \bar{f} = 0. \tag{7}$$

In equation (5), the Cauchy stress tensor σ is defined through an hyperelastic model (Ponthot et al. (2005)) where ψ^e is the elastic free energy function defined later in equation (8). Equation (6) describes the flow rule where, similarly as in the elastoplastic model, λ^{vp} is the viscoplastic multiplier, and n denotes the unit outward normal to the yield surface ($n : n = 1$).

2.3 Viscoplastic model for metals

Elastic strains are small for metals under large strains (Simo and Hughes (1998)). In this case the tensor F^e approaches to the Identity. Consequently tensor b^{e-1} tends to the spatial metric tensor g. In this case it is possible to write the elastic component of the free energy function as a quadratic function of the elastic component of Almansi strain tensor e^e and material constants λ and μ, as shown in equation (8) (García Garino (1993)).

$$\psi^e = \left[\frac{1}{2} \lambda \, tr(e^e)^2 + \mu \, (e^e : e^e) \right], \tag{8}$$

The expression for ψ^e has been used by García Garino (1993); García Garino and Oliver (1995, 1996) as an alternative to the neohookean models proposed by another authors (Simo (1988a,b); Simo and Ortiz (1985)).

Replacing equation (8) in (5) the Cauchy stress tensor results

$$\sigma = \lambda \, tr(e^e) \, 1 + 2 \, \mu \, e^e. \tag{9}$$

The yield stress σ_y is assumed for an isotropic linear hardening of the material as

$$\sigma_y = \sigma_{y0} + h\bar{\epsilon}^{vp}, \tag{10}$$

where h is the strain hardening modulus and σ_{y0} is the initial yield stress. The effective stress $\bar{\sigma}$ is a function of the deviatoric stress tensor $\boldsymbol{s}$,

$$\bar{\sigma} = \sqrt{\frac{3}{2} \boldsymbol{s} : \boldsymbol{s}}. \tag{11}$$

The viscoplastic multiplier rate $\dot{\lambda}^{vp}$ and the generalized yield function $\bar{f}$ have been defined by Ponthot (2002) including in the viscoplastic model the overstress d,

$$d = \langle \bar{\sigma} - \sigma_y \rangle , \tag{12}$$

where $\langle x \rangle$ denotes the Mac Auley brackets. For this viscoplastic model, contrary to the case of rate independent plasticity, the effective stress $\bar{\sigma}$ is no longer constrained to remain less or equal to the yield stress σ_y. Then it is possible that $\bar{\sigma} \geq \sigma_y$ and $d \neq 0$.

The expression for the viscoplastic multiplier rate $\dot{\lambda}$ developed by Ponthot (2002) is an increasing function of the overstress d, i.e.

$$\dot{\lambda}^{vp} = \sqrt{\frac{3}{2}} \left\langle \frac{\bar{\sigma} - \sigma_y}{\eta (\bar{\epsilon}^{vp})^{1/n}} \right\rangle^m , \tag{13}$$

where n is a hardening exponent, m is a rate sensitivity parameter, and η is a viscosity parameter. Clearly, an inelastic process can only take place if the overstress d is positive.

The kinematic variable $\bar{\epsilon}^{vp}$ is the equivalent to the effective plastic strain and its rate is defined as

$$\dot{\bar{\epsilon}}^{vp} = \sqrt{\frac{2}{3} \boldsymbol{d}^{vp} : \boldsymbol{d}^{vp}} . \tag{14}$$

Replacing the flow rule given in equation (6) into equation (14), the effective viscoplastic strain results

$$\dot{\bar{\epsilon}}^{vp} = \sqrt{\frac{2}{3}} \dot{\lambda}^{vp} . \tag{15}$$

Combining equations (13), and (15) gives

$$\dot{\bar{\epsilon}}^{vp} = \left\langle \frac{\bar{\sigma} - \sigma_y}{\eta (\bar{\epsilon}^{vp})^{1/n}} \right\rangle^m , \tag{16}$$

so that, in the viscoplastic range, the generalized yield function $\bar{f}$ has been defined as a new constraint (Ponthot (2002)),

$$\bar{f} = \bar{\sigma} - \sigma_y - \eta (\bar{\epsilon}^{vp})^{1/n} (\dot{\bar{\epsilon}}^{vp})^{1/m} = 0. \tag{17}$$

The criterion (17) is a *generalization of the classic von-Mises criterion* $f = 0$ *for rate-dependent materials.* The latter can simply be recovered by imposing $\eta = 0$ (no viscosity effect), result that has been pointed out in the literature by other authors (Alfano et al. (2001); Ottosen and Ristinmaa (2005); Wang and Sluys (2000)). In the elastic regime, both f and $\bar{f}$ are equivalent since in that case

$$\dot{\bar{\epsilon}}^{vp} = 0 \qquad \text{and} \qquad \bar{\sigma} \leq \sigma_y , \tag{18}$$

so that one has, similarly to plasticity,

$$\bar{f} \leq 0 . \tag{19}$$

Moreover, from relation (13), it can be noted, that as viscosity η goes to zero (rate-independent case), the viscoplastic multiplier $\dot{\lambda}^{vp}$ remains finite and positive (though indeterminate) since $(\bar{\sigma} - \sigma_y)$ also goes to zero. It allows a generalization of the Kuhn-Tucker which, in the viscoplastic case, can be extended as shown in equation (7).

3 NUMERICAL SCHEME

The numerical scheme, necessary to implement the discussed theoretical model in a finite element code, is based on an *elastic* predictor, *plastic* corrector approach, adapting the plastic variables to their viscoplastic counterparts. The elastic predictor scheme, common for both rate dependent and independent models, is presented in section 3.1 and plastic and viscoplastic correction schemes in sections 3.2 and 3.3 respectively.

The unknown whose value is necessary to perform the viscoplastic correction of the kinematic tensors, is the viscoplastic multiplier defined in equation (13). More specifically, it must be the solution of the generalized yield criterion (17). To solve that equation, its variables are discretized and its roots found by means of the Newton Raphson method due to the non-linear nature of the obtained equation.

Assuming a body on its initial state called 0, then moving through different states 1, 2,..., produced by increments of load, in accordance with times t_0, t_1 ..., where $t_{i+1} - t_i = \Delta t$, the unknowns of this problem are $^{t+\Delta t}\mathbf{s}$, $^{t+\Delta t}\bar{\varepsilon}^{vp}$ and $^{t+\Delta t}\sigma_y$ at the end of the interval.

3.1 Elastic Problem

In this problem the plastic quantities remain frozen, i.e. $^{t+\Delta t}\boldsymbol{F}^{pTR} = {}^{t}\boldsymbol{F}^p$. The trial *elastic* component of the deformation gradient tensor results:

$$^{t+\Delta t}\boldsymbol{F}^{eTR} = {}^{t+\Delta t}\boldsymbol{F} \ (^{t+\Delta t}\boldsymbol{F}^{pTR})^{-1} = \boldsymbol{f} \ {}^{t}\boldsymbol{F} \ (^{t}\boldsymbol{F}^p)^{-1} = \boldsymbol{f} \ {}^{t}\boldsymbol{F}^e, \tag{20}$$

where $\boldsymbol{f}$ is the incremental deformation gradient tensor. The predictor value of the elastic Finger tensor $^{t+\Delta t}\boldsymbol{b}^{e-1\,TR}$ is

$$^{t+\Delta t}\boldsymbol{b}^{e-1\,TR} = \left(^{t+\Delta t}\boldsymbol{F}^{e-T} \ {}^{t+\Delta t}\boldsymbol{F}^{e-1}\right)^{TR} = \boldsymbol{f}^{-T} \ {}^{t}\boldsymbol{b}^{e-1} \ \boldsymbol{f}^{-1}. \tag{21}$$

Finally, the trial stresses $\boldsymbol{\sigma}^{TR}$ are computed from equation (21) in terms of the predictor value of elastic Almansi strain $^{t+\Delta t}\boldsymbol{e}^{eTR} = \frac{1}{2}(^{t+\Delta t}\boldsymbol{g} \ - \ {}^{t+\Delta t}\boldsymbol{b}^{e-1\,TR})$.

3.2 Plastic Problem

In this problem the current configuration remains fixed and the internal variables are updated in order to satisfy the constitutive law. For this problem Simo (1988b) has proposed to integrate the flow rule in the original configuration. The pull-back operation of the right Cauchy Green tensor $\boldsymbol{C}^p$ is shown below in equation (22),

$$\dot{\boldsymbol{C}}^p = 2\phi^*\boldsymbol{d}^p = 2\dot{\lambda}^p\phi^*\boldsymbol{n} = 2\dot{\lambda}^p\boldsymbol{N} \tag{22}$$

where ϕ^* denotes the pull-back operator (Marsden and Hughes (1983)) which when applied to the unit outward normal $\boldsymbol{n}$ to the yield surface in the Cauchy stress space gives the normal tensor

N to the yield surface in the second Piola-Kirchhoff stress space. Equation (22) is integrated using a Backward-Euler scheme,

$$^{t+\Delta t}\boldsymbol{C}^p - {}^t\boldsymbol{C}^p = 2\lambda^p \; {}^{t+\Delta t}\boldsymbol{N}, \tag{23}$$

Pushing equation (22) towards the spatial configuration, the updated Finger tensor is found:

$$^{t+\Delta t}\boldsymbol{b}^{e-1} = {}^{t+\Delta t}\boldsymbol{b}^{e-1\,TR} + 2\lambda^p \; {}^{t+\Delta t}\boldsymbol{n} \tag{24}$$

The factor $2\lambda^p \; {}^{t+\Delta t}\boldsymbol{n}$ is computed by mean of the radial return algorithm.

3.3 Viscoplastic Problem

Viscoplastic counterpart of rate independent problem presented in previous section can be written in terms of viscoplastic component of right Cauchy Green tensor $\dot{\boldsymbol{C}}^{vp}$. Numerical plastic multiplier has been denoted λ^{vp} for this problem.

$$\dot{\boldsymbol{C}}^{vp} = 2\phi^*\boldsymbol{d}^{vp} = 2\dot{\lambda}^{vp}\phi^*\boldsymbol{n} = 2\,\dot{\lambda}^{vp}\boldsymbol{N} \tag{25}$$

Following the same steps of plastic corrector the updated figer tensor is computed as:

$$^{t+\Delta t}\boldsymbol{b}^{e-1} = {}^{t+\Delta t}\boldsymbol{b}^{e-1\,TR} + 2\lambda^{vp} \; {}^{t+\Delta t}\boldsymbol{n} \tag{26}$$

From equations (24) and (26) follows that both updates are identical with the exception of plastic multiplier λ^p and viscoplastic multiplier λ^{vp}. Consequently the structure of the numerical problem is preserved and rate dependent case is naturally encompassed as a particular case of corrector step.

From equation (4) the elastic component of Almansi strain tensor results in terms of the viscoplastic update of elastic Finger tensor given in equation (26):

$$
\begin{aligned}
^{t+\Delta t}\boldsymbol{e}^e &= \frac{1}{2}(g - {}^{t+\Delta t}\boldsymbol{b}^{e-1}) = \\
&= \frac{1}{2}(g - {}^{t+\Delta t}\boldsymbol{b}^{e-1\,TR} - 2\lambda^{vp} \; {}^{t+\Delta t}\boldsymbol{n}) = \\
&= {}^{t+\Delta t}\boldsymbol{e}^{e\,TR} - \lambda^{vp} \; {}^{t+\Delta t}\boldsymbol{n}
\end{aligned}
\tag{27}
$$

Taking into account equation (9), the viscoplastic correction of the elastics component of Almansi strain tensor given in equation (27) is written in terms of Cauchy stress tensor as:

$$^{t+\Delta t}\boldsymbol{\sigma} = {}^{t+\Delta t}\boldsymbol{\sigma}^{TR} - 2\lambda^{vp}\mu^{t+\Delta t}\boldsymbol{n} \tag{28}$$

that is the result shown in equation (51), section 6.3 in the work of Ponthot (2002), after integration over the time interval $[t, t + \Delta t]$, with initial conditions given by ${}^t\boldsymbol{\sigma}$, ${}^t\bar{\epsilon}^{vp}$ and ${}^t\sigma_y$.

3.4 Discrete consistency equation

Considering the generalized yield criterion $\bar{f} = 0$ given in equation (17) at time $t + \Delta t$,

$$\bar{f} = {}^{t+\Delta t}\bar{\sigma} - {}^{t+\Delta t}\sigma_y - \eta\big({}^{t+\Delta t}\bar{\epsilon}^{vp}\big)^{1/n}\big({}^{t+\Delta t}\dot{\bar{\epsilon}}^{vp}\big)^{1/m} = 0 \,. \tag{29}$$

it ensures the compliance of the *generalized consistency condition* (Ponthot (2002)) at that time.

The effective viscoplastic strain can be expressed in an incremental way as ${}^{t+\Delta t}\bar{\epsilon}^{vp} = {}^{t}\bar{\epsilon}^{vp} + \Delta\bar{\epsilon}^{vp}$ and in the same way equation (15) leads to $\Delta\bar{\epsilon}^{vp} = \sqrt{\frac{2}{3}}\lambda^{vp}$. Combining this last two expressions, the effective viscoplastic strain results

$$
{}^{t+\Delta t}\bar{\epsilon}^{vp} = {}^{t}\bar{\epsilon}^{vp} + \sqrt{\frac{2}{3}}\lambda^{vp}. \tag{30}
$$

where the (unknown) scalar parameter λ^{vp} stands for

$$
\lambda^{vp} = \int_{t}^{t+\Delta t} \dot{\lambda}^{vp} \ dt \tag{31}
$$

A replacement of equation (30) into the expression of the current yield stress given in equation (10) leads to

$$
{}^{t+\Delta t}\sigma_y = {}^{t}\sigma_y + h\sqrt{\frac{2}{3}}\lambda^{vp} . \tag{32}
$$

The predictor/corrector method is used with the radial return mode, it is,

$$
{}^{t+\Delta t}\boldsymbol{s} = {}^{t+\Delta t}\boldsymbol{s}^{TR} - 2\mu \ {}^{t+\Delta t}\lambda^{vp} \ {}^{t+\Delta t}\boldsymbol{n} , \tag{33}
$$

where ${}^{t+\Delta t}\boldsymbol{n}$ is computed as a function of deviatoric components of the predictor stress tensor as

$$
{}^{t+\Delta t}\boldsymbol{n} = \frac{{}^{t+\Delta t}\boldsymbol{s}^{TR}}{\sqrt{{}^{t+\Delta t}\boldsymbol{s}^{TR} : {}^{t+\Delta t}\boldsymbol{s}^{TR}}} . \tag{34}
$$

Finally, considering obtained equations (30), (32) and (33) the equation (29) can be rewritten as

$$
\begin{aligned}
\bar{f}(\lambda^{vp}) = &\sqrt{\frac{3}{2}\left[{}^{t+\Delta t}\boldsymbol{s}^{TR} - 2\mu \, \lambda^{vp \, t+\Delta t}\boldsymbol{n}\right] : \left[{}^{t+\Delta t}\boldsymbol{s}^{TR} - 2\mu \, \lambda^{vp \, t+\Delta t}\boldsymbol{n}\right]} + \\
&- {}^{t}\sigma_y + h\sqrt{\frac{2}{3}}\lambda^{vp} - \eta \left({}^{t}\bar{\epsilon}^{vp} + \sqrt{\frac{2}{3}}\lambda^{vp}\right)^{\frac{1}{n}} \left(\sqrt{\frac{2}{3}}\frac{\lambda^{vp}}{\Delta t}\right)^{\frac{1}{m}} = 0, \tag{35}
\end{aligned}
$$

that is the the generalized yield criterion on its discrete version, whose only unknown is λ^{vp}.

3.5 Numerical solution of discrete generalized yield criterion

The expression (35) is a non-linear equation in λ^{vp}, and it can be solved with a Newton-Raphson scheme, as was pointed out by Andia Fages (2010); Andia Fages et al. (2009) for a local problem, by Castelló and Flores (2010) in a Finite Element context as well as Ribero Vairo et al. (2011) who appealed to the False Position method to overcome the non-convergence obstacles. This latter scheme is used in this work, with a relative error tolerance of $1e(-3)$.

3.6 Particular cases

Considering the equation given in (29), special cases can be obtained depending on values of parameters m, n and η. More details about special cases can be seen in works of Ponthot (2002) and Andia Fages (2010); Andia Fages et al. (2009). Some of them are detailed below and discussed their numerical results latter in section 4 of numerical examples.

1. Non-viscous effects

   (a) Elastoplastic case, $\eta = 0$

   The classic elastoplastic case is recovered by setting $\eta = 0$. The generelized yield criterion given in equation (29) leads to

   $$\bar{f} = {}^{t+\Delta t}\bar{\sigma} - {}^{t+\Delta t}\sigma_y = 0. \tag{36}$$

   If considering the fully discretized expression for $\bar{f}$ in terms of the unknown λ^{vp} given in equation (35), a closed form solution identical to the plastic multiplier λ^p can be found (Ponthot (2002)),

   $$\lambda^{vp} = \lambda^p = \frac{1}{2\mu} \frac{|\boldsymbol{s}^{TR}| - \sqrt{\frac{2}{3}}\,{}^t\sigma_y}{\left(1 + \frac{h}{3\mu}\right)} . \tag{37}$$

   (b) Elastic problem, $\eta \to \infty$

   When the viscosity parameter tends to infinity, the viscous effect increases as well. Then, the effective stress can take any value without bounding yield surface and the behaviour tends to the elastic case.

2. Elasto viscoplastic problems

   To understand the effect of parameters m and n two cases of non-linear viscoplasticity can be studied:

   (a) Non-multiplicative hardening, $n \to \infty$: in this case the viscoplastic behaviour is controlled exclusively by the viscoplastic strain rate. Considering equation (29) as a function and taking the limit for $n \to \infty$, the generalized yield criterion turns to

   $$\bar{f} = {}^{t+\Delta t}\bar{\sigma} - {}^{t+\Delta t}\sigma_y - \eta\big({}^{t+\Delta t}\dot{\bar{\epsilon}}^{vp}\big)^{1/m}, \tag{38}$$

   where the last term represents the viscous effect. For a fixed value of ${}^{t+\Delta t}\dot{\bar{\epsilon}}^{vp} \leq 1$, the viscous term is an increasing function of the sensitivity parameter m. Its extreme values can be identified by taking the proper limits,

   $$\lim_{m \to +\infty} \eta\big({}^{t+\Delta t}\dot{\bar{\epsilon}}^{vp}\big)^{1/m} = \eta\,, \tag{39}$$

   $$\lim_{m \to 1} \eta\big({}^{t+\Delta t}\dot{\bar{\epsilon}}^{vp}\big)^{1/m} = \eta\,\, {}^{t+\Delta t}\dot{\bar{\epsilon}}^{vp}. \tag{40}$$

   It means that the viscous effect is restricted in the upper limit to the value of η and in the lower as a fraction of η given for $\dot{\bar{\epsilon}}^{vp}$. Then, the parameter m regularize the effect of η.

(b) Unitary rate sensitivity parameter $m = 1$: in this case minimum effect of viscoplastic strain rate is achieved. Equation (29) turns to:

$$\bar{f} = {}^{t+\Delta t}\bar{\sigma} - {}^{t+\Delta t}\sigma_y - \eta({}^{t+\Delta t}\bar{\epsilon}^{vp})^{1/n} \; {}^{t+\Delta t}\dot{\bar{\epsilon}}^{vp} = 0 \tag{41}$$

Again, the viscous term $\eta({}^{t+\Delta t}\bar{\epsilon}^{vp})^{1/n} \; {}^{t+\Delta t}\dot{\bar{\epsilon}}^{vp}$ behaves as an increasing function of the hardening exponent n, if and only if ${}^{t+\Delta t}\bar{\epsilon}^{vp} \leq 1$. The extreme values are founded by taking the limits

$$\lim_{n \to +\infty} \eta({}^{t+\Delta t}\dot{\bar{\epsilon}}^{vp})({}^{t+\Delta t}\bar{\epsilon}^{vp})^{1/n} = \eta \; {}^{t+\Delta t}\dot{\bar{\epsilon}}^{vp}, \tag{42}$$

$$\lim_{n \to 1} \eta({}^{t+\Delta t}\dot{\bar{\epsilon}}^{vp})({}^{t+\Delta t}\bar{\epsilon}^{vp})^{1/n} = \eta \; {}^{t+\Delta t}\dot{\bar{\epsilon}}^{vp} \; {}^{t+\Delta t}\bar{\epsilon}^{vp}. \tag{43}$$

Then, the viscous term will vary between the viscosity parameter η value and a fraction of it, given by the product ${}^{t+\Delta t}\dot{\bar{\epsilon}}^{vp} \; {}^{t+\Delta t}\bar{\epsilon}^{vp}$.

4 NUMERICAL EXAMPLES

In order to validate the implementation of the viscoplastic model on the **SOGDE3D** code using H1/P0 elements, the problem of a 3D plate with a hole subjected to plane strain state was solved, comparing the results with previous ones obtained with **SOGDE2D** by Ribero Vairo et al. (2011).

New results are shown for other plane strain state problem, the GRECO project cantilever beam considering different values of the viscoplastic parameters.

4.1 Plate with a hole

The problem consists of a plain strain state rectangular plate of 20m x 36m with a 5m radius hole in its centre. Only a quarter of the sample is modelled due to symmetry of loads and geometry, using appropriate boundary conditions. The finite element mesh is shown in figure 1. While one element is used in the plate thickness, N elements are used at the top and lateral boundaries and $2N$ in the circumference sector. Three different meshes have been considered with N equal to 6, 12 and 24 elements. In figure 1 the $N = 12$ mesh is shown.

The plate is loaded by prescribed displacements in 400 steps of 0.005m at intervals of 1s, on its upper face, leading a large strain case, which is the same case tested by García Garino et al. (2006) for *linear viscoplasticity* ($m = 1$, $n \to \infty$) and Ribero Vairo et al. (2011) for other m and n values with **SOGDE2D**. The latter work is the source of reference results for this work. The analysed viscous case has a unitary rate sensitivity parameter and a hardening exponent equal three ($m = 1$, $n = 3$). The material properties are detailed in table 1.

Load-displacement curves are shown in figure 2a for limiting elastic cases, and in 2b for limiting elastoplastic cases. The abscissa axis contains the prescribed displacement, and in ordinate axis the sum of vertical reactions obtained on each step. Lines were used for **SOGDE3D** and points for **SOGDE2D**. For a better comparison only one every 10 point is plotted for **SOGDE2D** results.

On the one hand, from figure 2a a small difference between 2D and 3D curves is noted for high values of η, but an exact matching for elastic response. That difference is appreciated in

E	=	$2.1e5$MPa
ν	=	0.30
σ_{y0}	=	240MPa
h	=	0

Table 1: Plate with a hole. Material properties.
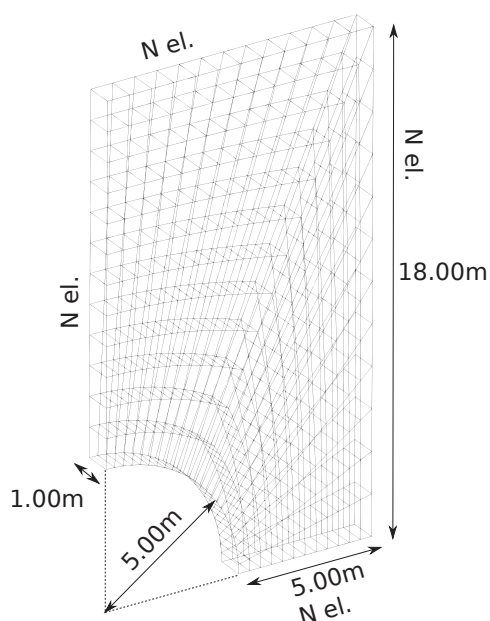
Figure 1: Plate with a hole. Geometry and finite element model.

large strain stage. On the other hand, 3D results presented in figure 2b are consistent with those obtained by 2D version of **SOGDE** code.

The expected behaviour was correctly simulated: limiting elastic and elastoplastic responses are recovered for large (higher than 1e9MPa·s) and small (lower than 1e4MPa·s) values of the viscoplastic parameter, respectively. A spectrum of responses can be obtained with intermediate values of η getting a softening response for small values of η.

In figures 3a and 3b deformed shapes for those extreme values of the viscous parameter are shown ($\eta = 1e4$MPa·s and $\eta = 1e9$MPa·s respectively). The influence of the viscoplastic parameter is also advised through the geometric effects presented after the deformation. The limiting elastoplastic response presents a remarkable necking effect, given by the pronounced slope of sides, in the narrow section of the plate. That non-linear geometric effect causes the softening response seen in figure 2b. The change of shape is copied by the elements which lose strongly their original aspect ratio. This leads convergence problem in larger prescribed displacements. In the other hand the behaviour of the plate for $\eta = 1e9$MPa·s dos not present strong changes of shape. Contrary to the elastoplastic limiting case no necking is noted, but a flattening of the hole sector is developed. In no case displacements were found perpendicular to the plate plane, given the plane strain state.

As a way to detect the mesh sensitivity over the response of the plate when a viscoplastic material is considered, three 3D mesh densities are studied given by $N = 6$, 12 and 24 giving a total of 64, 288 and 1152 elements respectively. Many values of the viscoplastic parameter η are considered taking the same values as in figures 2a and 2b. The results are presented in figures 4a for limiting elastic cases and in 4b for limiting elastoplastic cases. Each set of curves presents slight differences among them with a tendency of a greater dispersion when η decrease, where the non-linear geometric effects become significant. The number of iterations employed by each mesh density, in general, increases as η decreases, meaning that the approach to the elastoplastic response and the consequent development of viscoplastic deformations makes the implicit solver scheme more difficult to get convergence. Although the denser mesh requires more iterations to find the global convergence, it provides the best performance in terms of
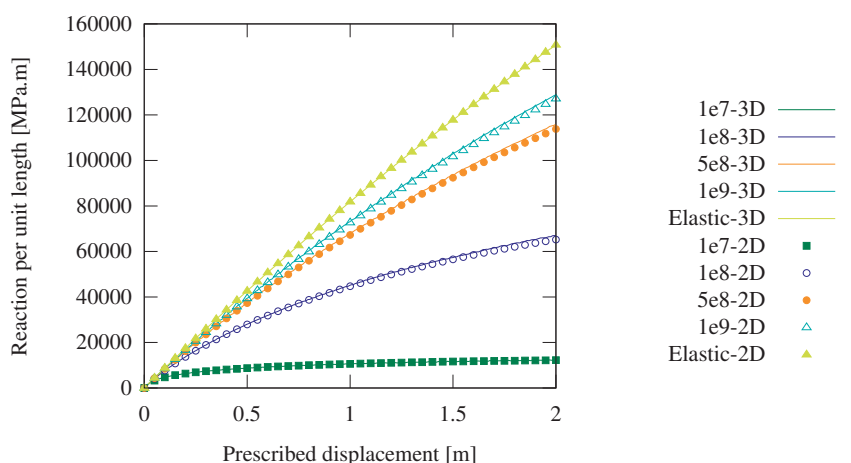
(a) Limiting elastic cases
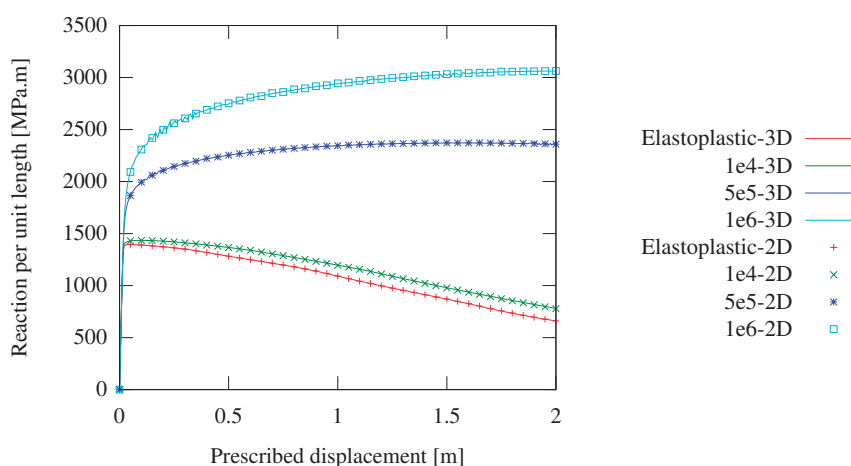
(b) Limiting elastoplastic cases

Figure 2: Plate with a hole. Obtained responses with **SOGDE2D** and **3D** for different values of η[MPa·s] when $m = 1$ and $n = 3$.

smoothness of the response curves. Response curves for the less dense mesh shows some noticeable numerical instabilities but no difficulties in the rate of convergence were found for any value of η. Finally, in relative terms of number of iterations and accuracy of solution it can be confirmed that the 288 elements mesh presents an acceptable behaviour.

4.2 GRECO beam bending

The GRECO beam problem was introduced as a benchmark by the GRECO project dedicated to finite strain and damage. It consists of a cantilever beam of 3mm length, 1mm height and 0.25mm thickness as shown in figure 5. It is subjected to a plain strain state with downwards displacements applied in 80 steps of 0.0125mm every 1s on its upper right corner. The finite element model consists of 48 H1/P0 elements placed in a single layer. The material properties are detailed in table 2. Also a sketch of geometry and mesh are showed in figure 5.

As was pointed out in section 3.6, null value of η allows to recover elastoplastic behaviour. Then, as an extra validation of the implementation, stress tensor components (σ_x, σ_y, σ_z and $|\sigma_{xy}|$)

(a) $\eta = 1e4$Mpa·s　　　　(b) $\eta = 1e9$Mpa·s
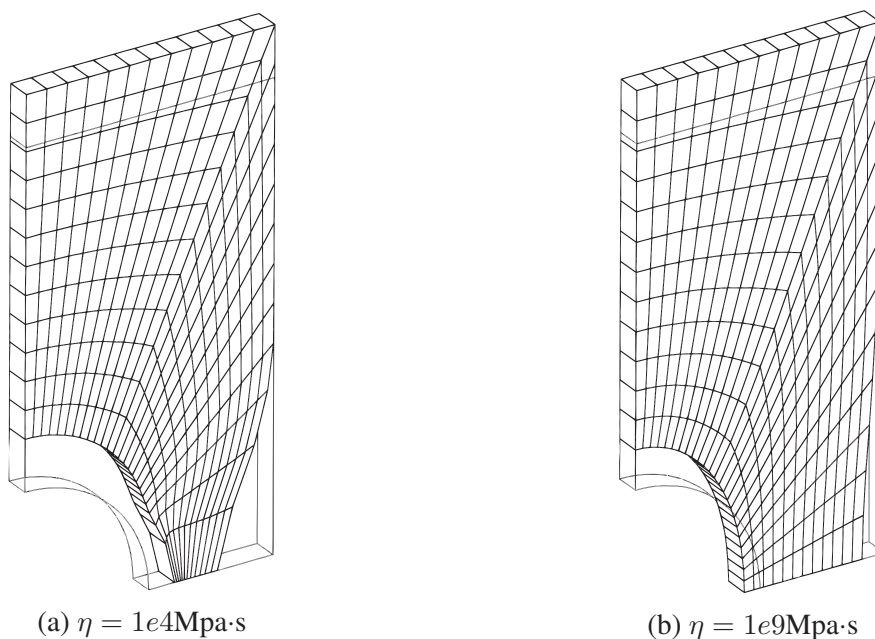
Figure 3: Final deformed shape for viscous cases with $m = 1$, $n = 3$ and extreme values of η.

(a) Limiting elastic cases　　　　(b) Limiting elastoplastic cases
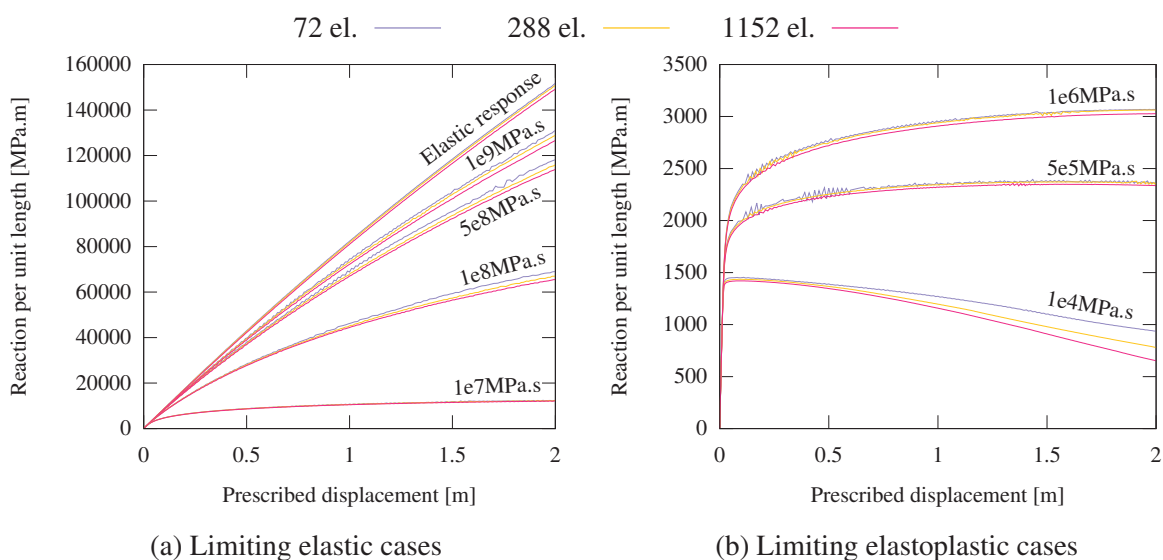
Figure 4: Sensitivity of response for different mesh densities

E	=	$2.0e5$MPa
ν	=	0.30
σ_{y0}	=	400MPa
h	=	1000MPa

Table 2: GRECO beam. Material properties.
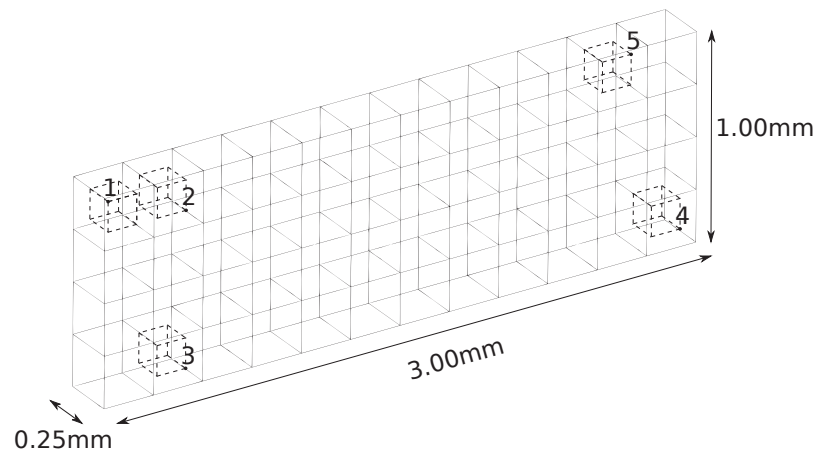
Figure 5: GRECO beam. Geometry and finite element model.

and effective plastic strain ($\bar{\epsilon}^p$) for the non-viscous case are contrasted at gauss point level, with results obtained in other previous work (see table 3). Results from Cao (1990) and Ponthot (1995) were extracted from a compilation made by El Mouatassim (1989). The five gauss points chosen are identified in figure 5 and, as was pointed out by García Garino (1993), the kinematic conditions on each gauss point are different: large strain and small rotation for point 1, points 2 and 3 present large strain and moderate rotation, point 4 large rotation and small strain and point 5 large displacement and rotation. Obtained results by this work presents a good accordance with the reference ones, with an excellent match with the work of Careglio et al. (2005).

Different viscoplastic responses of GRECO beam were reached using different combination of viscoplastic parameters. The obtained results are shown in figure 6 for non-multiplicative hardening ($n = 1e40$ to represent an infinit value) and in figure 7 for unitary rate sensitivity parameter ($m = 1$).

As shown in section 3.6, as the viscosity coefficient η increases, the response gets closer to the supposed elastic behaviour for the beam when $\sigma_y \to \infty$. From the plotted elastic response of the GRECO beam, a convexity can be detected for the finals displacements despite there is no development of viscoplastic strain in any point of the solid. That is due to the non-linear geometry effects considered by the large strain model. On the other hand, as η decreases, the response tends to an elastoplastic behaviour, where the softening effect is developed.

As m and n increase, the responses become stiffer, not only in cases of non-multiplicative hardening but also in unitary rate parameter. For example, observing curves of figures in 7a, 7b, 7c and 6a where $m = 1$ in all of them and n gets values of 1, 2, 3 in the first three and ∞ in the last one. It can be seen the regulatory character of the n parameter over the viscous effect. The response of the beam varies between two limiting curves corresponding to $n = 1$ and $n \to \infty$. When $\eta = 1e6$MPa·s the spectrum of curves goes from the response curve with 190MPa· mm of final reaction to a stiffer one with 850MPa· mm without reaching the elastic case.

But the effect of the m and n parameters is uneven for every value of η. In the non-multiplicative hardening case with $\eta = 1e3$MPa·s, the final reaction amounts to 64MPa·mm for $m = 1$ and to 196MPa·mm for $m = 3$. On the other hand when $\eta = 1e5$MPa·s a 216MPa·mm final reaction is reached for $m = 1$ and 1360MPa·mm for $m = 3$. This means an increase of 206% when $\eta = 1e3$MPa·s, against 530% when $\eta = 1e5$MPa·s in the final reaction. The same uneven effectiveness is appreciated for the n parameter, as can be seen in the unitary rate sensitivity parameter case, displayed in figure 7. The model responses obtained for $\eta \leq 1e4$MPa·s

Gauss Point	Code	σ_x	σ_y	σ_z	$|\sigma_{xy}|$	$\bar{\epsilon}^p$
1	This work	68.58	-3.73	32.61	5.80	0.2342
	Careglio et al. (2005)	68.58	-3.71	32.61	5.81	0.2341
	García Garino (1993)	68.58	-3.66	32.66	5.80	0.2337
	Ponthot (1995)	68.93	-3.72	32.66	5.78	0.2372
	Cao (1990)	66.19	-3.69	31.42	5.70	0.2559
2	This work	60.27	-0.10	30.67	11.59	0.1601
	Careglio et al. (2005)	60.26	-0.12	30.67	11.57	0.1601
	García Garino (1993)	60.33	-0.06	30.69	11.61	0.1650
	Ponthot (1995)	60.49	-0.01	30.74	11.71	0.1619
	Cao (1990)	57.92	0.52	29.29	11.75	0.1646
3	This work	-66.15	-0.61	-25.84	16.53	0.2402
	Careglio et al. (2005)	-66.18	-0.58	-25.86	16.47	0.2402
	García Garino (1993)	-66.28	-0.77	-25.97	16.71	0.2399
	Ponthot (1995)	-65.92	-1.04	-25.78	16.71	0.2367
	Cao (1990)	-60.98	-2.24	-27.35	15.72	0.2543
4	This work	-4.47	-1.33	-1.03	1.76	0.000
	Careglio et al. (2005)	-4.48	-1.34	-1.03	1.76	0.000
	García Garino (1993)	-4.49	-1.33	-1.01	1.75	0.000
	Ponthot (1995)	-4.42	-1.31	-1.03	1.75	0.000
	Cao (1990)	-3.71	-1.06	18.55	1.03	0.000
5	This work	28.44	3.86	-2.55	8.98	0.0482
	Careglio et al. (2005)	28.07	4.37	-2.56	9.30	0.0481
	García Garino (1993)	27.83	4.67	-2.55	9.43	0.0492
	Ponthot (1995)	28.78	3.13	-2.72	8.61	0.0482

Table 3: GRECO beam. Gauss points results comparison.

(a) $m = 1$

(b) $m = 2$

(c) $m = 3$
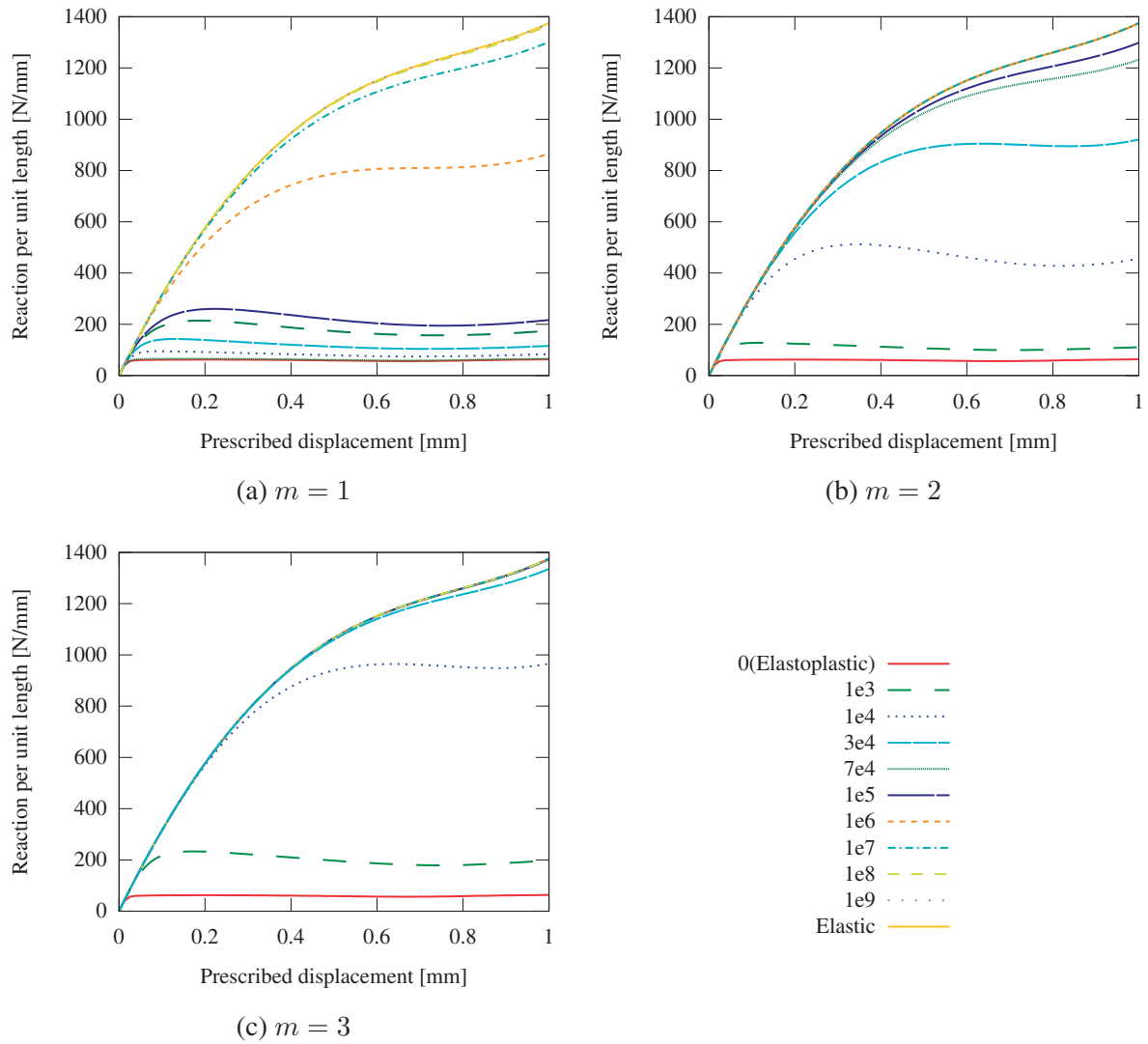
Figure 6: GRECO beam. Responses for different values of η[MPa·s] for non-multiplicative hardening, $n \to \infty$

(a) $n = 1$

(b) $n = 2$

(c) $n = 3$
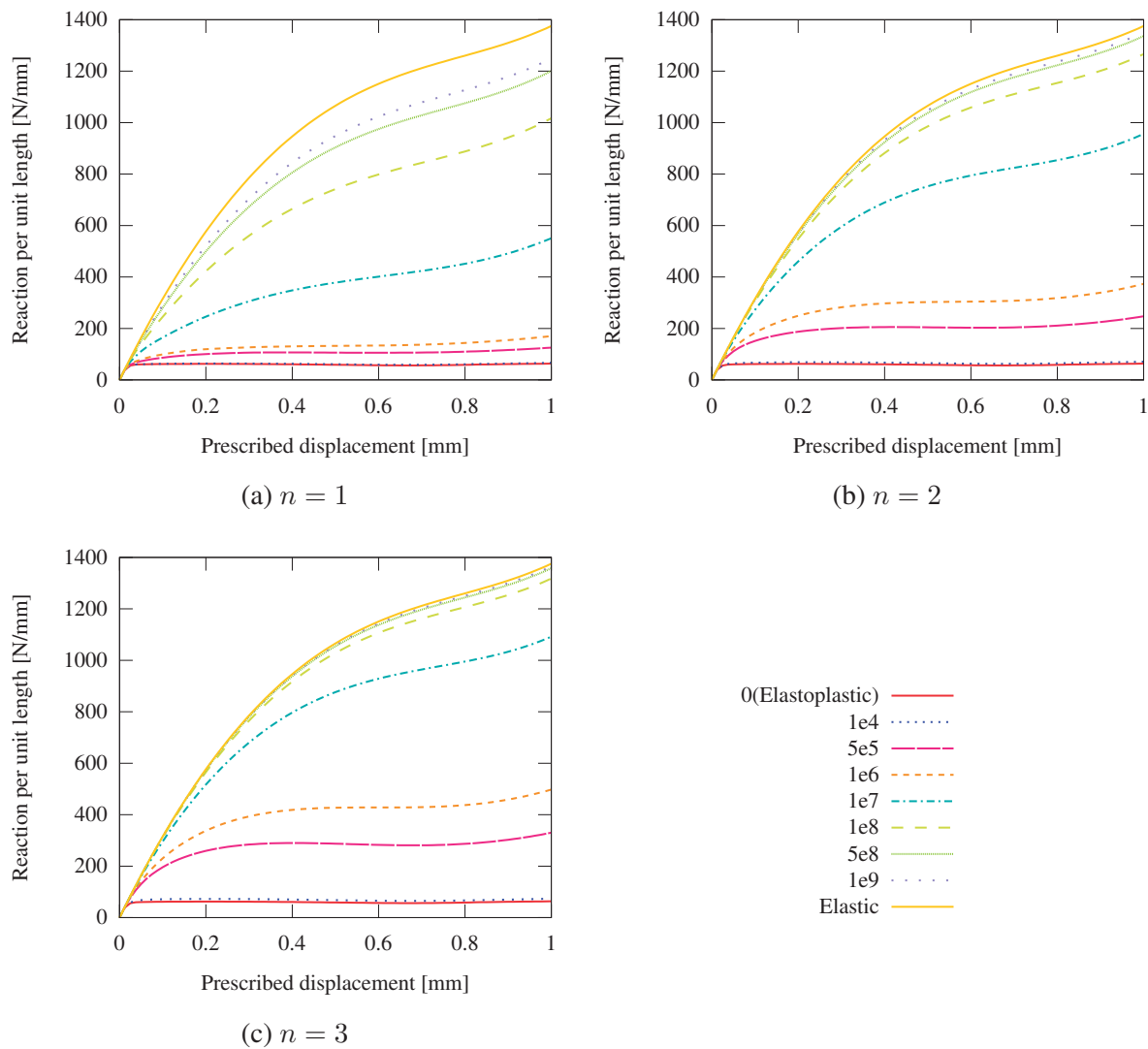
Figure 7: GRECO beam. Responses for different values of η[MPa·s] for unitary rate sensitivity parameter, $m = 1$

are quite insensitive to larger values of n. A similar analysis is derived for responses obtained with large values of η. The elastic response works as the stiffer possible limit of responses. So, as close responses to the elastic case can not increase in terms of reaction as m or n increases, the effectiveness of them decrease for high values of η.

Figure 8 shows the deformed meshes and the distributions of the effective viscoplastic strain for the non-multiplicative hardening case when $\eta = 1e4$ MPa·s and m takes values of 1, 2, and 3. The images were taken for the last prescribed displacement ($u = 1$mm). Although impossible to achieved for any m value when $\eta = 1e4$MPa·s, elastoplastic case was plotted in figure 8a just for reference purposes.

The contours of figures 8 shows that the development of the effective viscoplastic strain takes smaller values as the parameter m increases. On the contrary, the effective viscoplastic strain and its gradient appearing in the lower left hand side corner are higher as m decreases, tending to the elastoplastic configuration of contours shown in figure 8a. Also the deformation geometry changes as the m parameter increases. For $m = 1$, the deflection slope presents abrupt direction changes in the critical zones of higher viscoplastic strain values. This effect diminishes as m increases, reaching an almost smooth deflection for $m = 3$.


(a) Elastoplastic response ($\eta = 0$)   (b) $m = 1, n \to \infty, \eta = 1e4$MPa·$s$

(c) $m = 2, n \to \infty, \eta = 1e4$MPa·$s$ (d) $m = 3, n \to \infty, \eta = 1e4$MPa·$s$
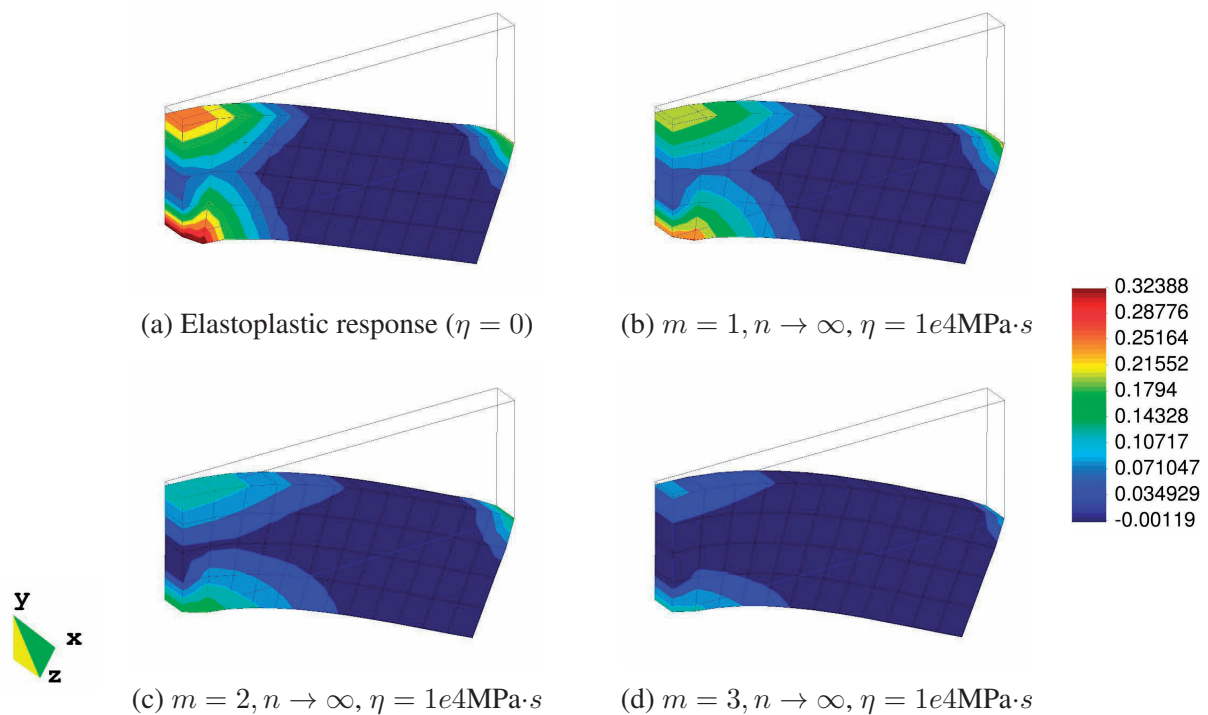
Figure 8: Viscoplastic effective strain at final deformed shape

5 CONCLUSIONS

A 3D large strain elasto viscoplastic model was presented and tested. The correct implementation of the model in **SOGDE3D** code was proved by comparison with previous results obtained with **SOGDE2D** in the analysis of the plate with a hole. For elastoplastic recovered case in the GRECO beam example, a gauss points level verification was performed considering available results in the literature.

The analysis of numerical examples with the implementation of the viscoplastic model confirmed the expected behaviour of the solid detailed in section 3.6, where the viscoplastic parameter η plays a role of a regularization parameter between the elastic and elastoplastic responses. The exponents n and m, in turn, regulate the effect of effective viscoplastic strain and its rate respectively, over the rate dependent behaviour of the material, in the same way as the viscosity parameter but constrained to a range of responses.

Both the plate with a hole and the GRECO beam example allow to interpret the effect of the m exponent over the deformed geometry. Typical elastoplastic and geometric nonlinearities are developed when $\eta = 1e4$MPa·s and the m parameter increases.

Also the effect of m and n parameters was assessed, concluding that no significant changes can be obtained when extreme values of the viscosity parameter η is considered.

REFERENCES

Alfano G., De Angelis F., and Rosati L. General solution procedures in elasto-viscoplasticity. *Computer methods in applied mechanics and engineering*, 190:5123–5147, 2001.

Andia Fages S. *Estudio de sensibilidad de la solución de la ecuación no lineal de consistencia de un modelo constitutivo elasto-viscoplástico*. Tesis de licenciatura en Matemáticas, Universidad del Aconcagua, Mendoza, Argentina, 2010.

Andia Fages S., Raichman S., Mirasso A., García Garino C., and Ponthot J. Integración numérica del problema viscoplástico. *Anales del V encuentro de investigadores y docentes de ingeniería*, pages 104–118, 2009.

Cao H. *Modelisation Méchanique et simulation numerique de l'emboutissage*. Ph.D. thesis, Instituto Nacional Politécnico de Grenoble, 1990.

Careglio C., García Garino C., and Mirasso A. Sogde3d: Código para elastoplasticidad con grandes deformaciones 3d. In A.E. Larreteguy, editor, *Mecánica Computacional*, volume XXIV, pages 363–373. Buenos Aires, Argentina, 2005. ISSN 1666-6070.

Castelló W. and Flores F. A triangular finite element with local remeshing for the large strain analysis of axisymmetric solids. *Computer Methods in Applied Mechanics and Engineering*, 198(2):332 – 343, 2008. ISSN 0045-7825. doi:10.1016/j.cma.2008.08.009.

Castelló W. and Flores F. Análisis de problemas elasto-viscoplásticos en conformado de metales. *Mecánica Computacional*, XXIX:4199–4217, 2010. ISSN 1666-6070.

El Mouatassim M. *Modelisation en grandes transformations des solides massifs par elements*. Ph.D. thesis, Université de technologie de Compiegne, France, 1989.

García Garino C. *Un modelo numérico para el análisis de sólidos elastoplásticos sometidos a grandes deformaciones*. Ph.D. thesis, Universidad Politécnica de Catalunya, Universidad Politécnica de Catalunya. Barcelona, España, 1993.

García Garino C. and Oliver J. Un modelo constitutivo para el análisis de sólidos sometidos a grandes deformaciones, parte i formulación teórica y aplicación a metales. *Revista Internacional de Métodos Numéricos para el Cálculo y Diseño en Ingeniería*, 11:105–122, 1995.

García Garino C. and Oliver J. Un modelo constitutivo para el análisis de sólidos sometidos a grandes deformaciones, parte ii implementación numérica y aplicaciones. *Revista Internacional de Métodos Numéricos para el Cálculo y Diseño en Ingeniería*, 12:147–169, 1996.

García Garino C., Ponthot J., Mirasso A., Koeune R., Jeunechamps P., and Careglio C. Numerical simulation of large strain rate dependent j2 problems. *Mecánica Computacional*, 25:1927–1946, 2006. ISSN 1666-6070.

García Garino C., Ribero Vairo M., Andía Fagés S., Mirasso A., and Ponthot J. Numerical simulation of finite strain viscoplastic problems. In M. Hogge, editor, *Fifth International*

Conference on Advanced COmputational Methods in ENgineering (ACOMEN 2011). Boman, R. and Ponthot, J.P., University of Liège, Liège, Belgium, 2011.

Lee E. Elastic-plastic deformation at finite strains. *Journal of Applied Mechanics*, 36:1–6, 1969.

Marsden E. and Hughes T. *Mathematical Foundations of Elasticity*. Prentice-Hall, 1983.

Ottosen N. and Ristinmaa M. *The Mechanics of Constitutive Modelling*. Elsevier, 2005.

Perzyna P. Fundamental problems in viscoplasticity. *Advances in Applied Mechanics*, 9(2):243–377, 1966.

Ponthot J. *Traitement unifie de la Mecanique des transformations pour la methode des elements finis*. Ph.D. thesis, Universite of Liège, Belgium, 1995.

Ponthot J. Unified stress update algorithms for the numerical simulation of large deformation elasto-plastic and elasto-viscoplastic processes. *International Journal of Plasticity*, 18:91–126, 2002.

Ponthot J., García Garino C., and Mirasso A. Large strain elasto viscoplastic constitutive model. Theory and numerical scheme. *Mecánica Computacional*, XXIV:441–454, 2005. ISSN 1666-6070.

Ribero Vairo M., van Hooijdonk J., Andia Fages S., Mirasso A., and García Garino C. Análisis de un modelo elasto-viscoplástico no-lineal. In O. Möller, J. Signorelli, and M. Storti, editors, *Mecánica Computacional*, volume XXX, pages 787–803. Facultad de Ciencias Exactas, Ingeniería y Agrimensura de la Universidad Nacional de Rosario, Rosario, Argentina, 2011. ISSN 1666-6070.

Simo J. A framework for finite strain elastoplasticity based on maximum plastic dissipation and the multiplicative decomposition: Part i. continuum formulation. *Computer Methods in Applied Mechanics and Engineering*, 66(2):199 – 219, 1988a. ISSN 0045-7825. doi: 10.1016/0045-7825(88)90076-X.

Simo J. A framework for finite strain elastoplasticity based on maximum plastic dissipation and the multiplicative decomposition. part ii: Computational aspects. *Computer Methods in Applied Mechanics and Engineering*, 68(1):1 – 31, 1988b. ISSN 0045-7825. doi:10.1016/0045-7825(88)90104-1.

Simo J. and Hughes T. *Computational Inelasticity*. Interdisciplinary applied mathematics: Mechanics and materials. Springer, 1998. ISBN 9780387975207.

Simo J. and Ortiz M. A unified approach to finite deformation elastoplastic analysis based on the use hiperelastic constitutive equation. *Computer Methods in Applied Mechanics Engineering*, 49:221–245, 1985.

Wang W.M. and Sluys L.J. Formulation of an implicit algorithm for finite deformation viscoplasticity. *International Journal of Solids and Structures*, 37:7329–7348, 2000.

Zienkiewicz O. and Taylor R. *El método de los elementos finitos*. McGraw-Hill, Interamericana de España, S.A., Madrid, España, 1994. ISBN 84-481-0178-2.